RSC Chemical Biology

Accepted Manuscript

This article can be cited before page numbers have been issued, to do this please use: K. K. Kung, Y. T. Limanto, A. Tantipanjaporn, J. Deng, L. Y. Tsang and M. K. Wong, *RSC Chem. Biol.*, 2025, DOI: 10.1039/D5CB00289C.

ROYAL SOCIETY OF CHEMISTRY

rsc.li/rsc-chembio

View Article Online
DOI: 10.1039/D5CB00289C

ARTICLE

Fluorescent Cationic Fluorinated Oxazoliniums for Cysteine Bioconjugation via S_NAr Reaction

Received 00th January 20xx,
Accepted 00th January 20xx

DOI: 10.1039/x0xx00000x

Karen Ka-Yan Kung,‡[a,b] Yosephine Tania Limanto,‡[a] Ajcharapan Tantipanjaporn,[a] Jie-Ren Deng,[c] Lai-Yi Tsang,[c] and Man-Kin Wong*[a,b]

Using cationic fluorinated oxazolinium compounds, fluorescent cysteine-selective S_NAr bioconjugation proceeds under mild conditions, resulting in fluorescent-labelled peptides and proteins with moderate to excellent conversions of up to 99%. Live cell imaging studies reveals good compatibility of these oxazoliniums as fluorescent dyes for mitochondrial targeting.

Introduction

Fluorescent labelling allows the attachment of fluorophores to biomolecules, resulting in fluorescent bioconjugates with excellent selectivity and functional diversity for visualizing and tracking in biological activities.[1-3] Cysteine is commonly used as a handle in bioconjugation due to its high nucleophilicity and relatively low abundance.[1, 4] Therefore, different classes of electrophiles, including *α,β*-unsaturated carbonyls, maleimides and hypervalent iodine compounds, have been developed for cysteine-based modification of peptides and proteins.

Cysteine arylation by fluorinated aromatic compounds *via* nucleophilic aromatic substitution (S_NAr) has demonstrated advantages over metal- or photo-catalyzed arylation.[5, 6] Since 2013, Pentelute *et al*.,[7, 8] Derda *et al*.,[9] Cobb *et al*.,[10] Wu *et al*.[11] and Harran *et al*.[12] developed polyfluoroaromatic compounds for cysteine-selective bioconjugation and Cys–Cys stapling of native peptides (Figure 1a). Recently, pyridinium salts, such as *N*-methyl-*o*-fluoropyridinium iodide (CAP1), showed excellent reactivity due to the cationic nature, water solubility and highly polarized C-F bonds towards rapid thiol arylation (Figure 1b).[13]

Various advancements have been made in fluorescence analysis using small-molecule fluorescent probes including the incorporation of fluorine to fluorophores to improve imaging capabilities, targeting functionalities and overall biological activities.[14-16] To achieve fluorescent cysteine bioconjugation, attachment of a fluorescent dye into the bioconjugation reagents is necessary, requiring additional synthetic effort. Thus, it is interesting to develop a fluorescent bioconjugation reagent without the need for addition of a separate fluorescent dye. Notably, Zhang *et al*. introduced a series of fluorescent polyfluoroporphyrins for labelling of cysteine-containing peptides and proteins *via* S_NAr reactions while preserving water solubility, cationic nature and tunable fluorescence (Figure 1c).[17]

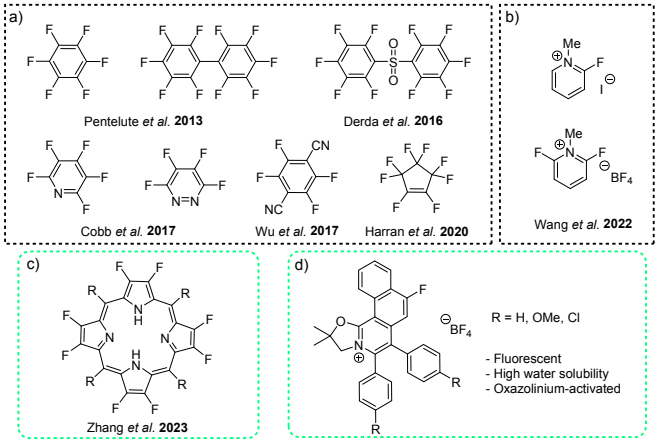

Figure 1. Fluorinated compounds for cysteine arylation. a) Polyfluoroaromatics compounds. b) Pyridinium-activated fluorine. c) Fluorescent polyfluoroporphyrin. d) Our fluorescent fluorinated oxazolinium compounds.

Although many cationic polycyclic heteroaromatics, such as isoquinoliniums, quinoliziniums, and pyridiniums have been reported as water-soluble fluorophores, very few reports are on the synthesis and applications of oxazoliniums.[18-20] Here, we report a series of fluorescent cationic fluorinated oxazoliniums for cysteine bioconjugation *via* S_NAr reaction (Figure 1d). By using rhodium (Rh)-catalyzed reaction, a series of fluorinated

[a] *Research Institute for Future Food, Department of Food Science and Nutrition, The Hong Kong Polytechnic University, Hung Hom, Hong Kong, China. Email: mankin.wong@polyu.edu.hk.*
[b] *Centre for Eye and Vision Research (CEVR), 17W Hong Kong Science Park, Hong Kong, China.*
[c] *Department of Applied Biology and Chemical Technology, The Hong Kong Polytechnic University, Hung Hom, Hong Kong, China.*
‡ These authors contributed equally to this work.
† Supplementary Information available: Details of experimental procedures, LC-MS analyses, DFT data and NMR data. See DOI: 10.1039/x0xx00000x

oxazolinium compounds were prepared using a modular approach.[21]

Investigation of the photophysical properties and applications of the fluorinated oxazoliniums for cysteine bioconjugation and live cell imaging were performed.

Results and discussion

Synthesis and Designing of Oxazoliniums

Based on our previous study on the development of polycyclic quinoliziniums[22-24] and oxazoliniums,[25] oxazolinium **oxa-1** was first synthesized *via* a Rh-catalyzed C–H annulation between oxazoline **S1a** and diphenylacetylene **S2a** in the presence of silver salt (Scheme 1). Oxazolinium **oxa-1** was characterized by NMR and mass spectrometry (ESI†).

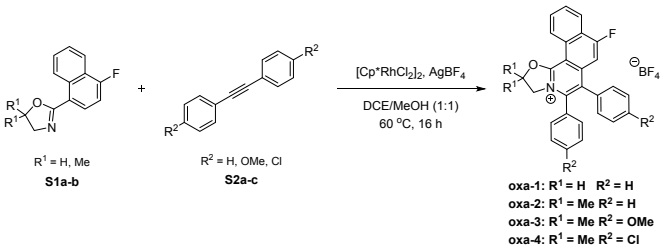

Scheme 1. Synthetic procedure of **oxa-1-4**.

We initiated the study through the reaction of **oxa-1** (10 equiv.) with cysteine-containing peptide **1** (STSSSCNLSK) (0.1 mM, 1 equiv.) for 18 h at room temperature (Scheme S1, ESI†). By utilization of LC-MS to determine the conversion, we found that reaction at room temperature led to a moderate conversion of 61% of modified peptide **1a** (Figure S13, ESI†). To improve the conversion, the reaction mixture was heated to 40 °C for 18 h. Unexpectedly, 75% of peptide **1** was converted to the hydrolysed product **1a'** (Figure S15, ESI†). In addition, dimerization of the native peptide **1** increased to 23% from 9% at room temperature. As the C2 carbon atom of the oxazoline is susceptible to nucleophilic attack,[26] **oxa-2-4** were designed with geminal dimethyl groups to overcome the hydrolysis of the target product.

Optimization of Peptide Modification Reaction Conditions

Treatment of the peptide **1** with **oxa-2** (10 equiv.) at room temperature gave a moderate conversion of 66% and 10% dimerization (Table 1, entry 1). Upon heating of the reaction mixture to 40 °C, a significant increase to 86% in conversion was observed (entry 2). As dimerization of the peptide was a competing reaction to the cysteine arylation, TCEP (a reducing agent) was added to inhibit the dimerization (entry 3). Optimization of the reaction conditions was conducted by screening different conditions and varying the amount of **oxa-2** and TCEP (entries 4-9). To our delight, up to 96% conversion was attained when only 5 equivalents of **oxa-2** and 1 equivalent of TCEP were utilized under heating at 40 °C (entry 7).

With the optimized conditions at hand, a time course study was conducted. Up to 95% conversion was obtained within 16 h of reaction before reaching an equilibrium (Figure S1, ESI†). Peptide **1** was then treated with electron-donating substituted **oxa-3** and electron-withdrawing substituted **oxa-4**, leading to 90% and 99% conversion respectively (entries 10-11). The higher conversion obtained from the electron-withdrawing **oxa-4** compared to **oxa-2** and **oxa-3** is possibly due to the higher electrophilicity of the cation due to the -Cl substituent. Furthermore, as proof of concept, no target product was observed when the peptide **1** was treated with oxazoline **S1b** as control (entry 12). This observation indicated that cysteine arylation is enhanced by the cationic nature of the oxazolinium electrophiles and highly polarized C–F bonds.[13]

Table 1. Optimization of cysteine arylation reaction conditions.[a]

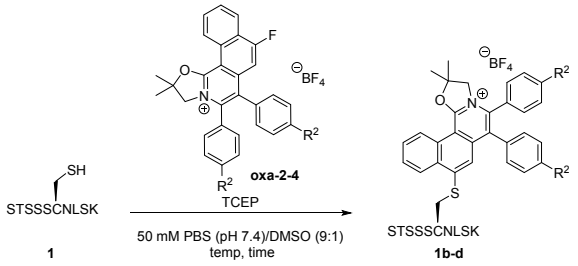

Entry	Compound (equiv.)	TCEP (equiv.)	Temp. (°C)	Time (h)	Product	Conv. (%)[b]
1	**oxa-2** (10)	0	rt	18	**1b**	66
2	**oxa-2** (10)	0	40	18	**1b**	86
3	**oxa-2** (10)	10	rt	18	**1b**	64
4	**oxa-2** (10)	10	40	18	**1b**	94
5	**oxa-2** (5)	5	40	18	**1b**	95
6	**oxa-2** (5)	2	40	18	**1b**	96
7	**oxa-2** (5)	1	40	18	**1b**	96
8	**oxa-2** (3)	1	40	18	**1b**	91
9	**oxa-2** (1)	1	40	18	**1b**	89
10[c]	**oxa-3** (5)	1	40	16	**1c**	90
11[c]	**oxa-4** (5)	1	40	16	**1d**	99
12[c]	**S1b** (Control) (5)	1	40	16	**1e**	0

[a] Reaction conditions for modification: Treatment of peptide **1** (0.1 mM) with **oxa-2** in the presence of TCEP, in 50 mM PBS buffer (pH 7.4)/DMSO (9:1). [b] Conversion of the modification was determined by LC-MS/MS analysis. [c] Optimized conditions following time-course study, **oxa-3**, **oxa-4** and oxazoline **S1b** utilized.

Model Reactions of Peptide Modifications

Model reactions were conducted by treatment of **oxa-2-4** (0.1 mmol, 1 equiv.) and *N*-Boc cysteine methyl ester (1.5 equiv.) at room temperature for 16 h to give **oxa-5-7** (Scheme 2). By using mass spectrometry, no starting **oxa-2-4** were observed in the crude mixture, indicating complete consumption of the starting oxazolinium compounds. However, difficulties in purification of the resulting products led to low isolated yields (accounting

only the purest fraction collected). Yet, the cysteine-arylated products **oxa-5-7** were successfully characterized by NMR and mass spectrometry (ESI†).

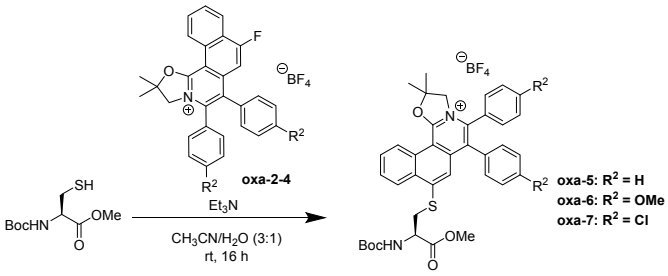

Scheme 2. Model reactions of cysteine arylation using *N*-Boc cysteine methyl ester.

Evaluation of Photophysical Properties and DFT Calculations

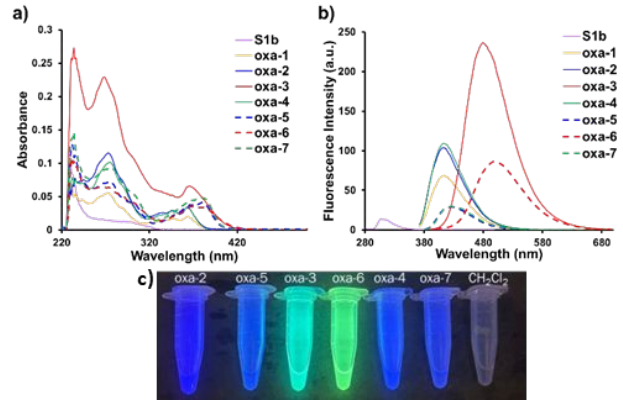

Figure 2. a) Absorption spectra, b) fluorescence spectra of oxazoline **S1b** and **oxa-1-7** (1 μM in CH_2Cl_2), c) fluorescence images of **oxa-2-7** and solvent (control) under a 365 nm UV lamp (1 mM in CH_2Cl_2).

As depicted in Figure 2 and Table 2, the photophysical properties of **oxa-1-7** and **S1b** were studied in CH_2Cl_2. **Oxa-1** (R^1 = H) caused a red-shift absorption and emission, higher molar absorptivity (ε), and greater fluorescence quantum yield (Φ_F) compared to the non-cationic **S1b** (entries 1-2). Comparing between **oxa-1** (R^1 = H) and **oxa-2** (R^1 = CH_3), the geminal methyl substituents of **oxa-2** demonstrated negligible effect on photophysical properties (entries 2-3). The electron donating -OMe group on R^2 of **oxa-3** gave the red-shift emission (480 nm), larger Stoke shifts, and highest Φ_F (0.51) (entry 4) while electron withdrawing -Cl group on R^2 of **oxa-4** showed similar photophysical properties to **oxa-2** (entry 5 vs entry 3). Thus, the substituents on R^2 showed significant effects on ε, emission, and Φ_F. In addition, the resulting **oxa-5-7** of the substitution of *N*-Boc cysteine methyl ester with **oxa-2-4** exhibited red-shift absorption and emission (entries 6-8). Notably, the bright fluorescence images of **oxa-3** and **oxa-6** imply the potential application of **oxa-3** in fluorescent labelling and bioimaging (Figure 2c). Moreover, the photophysical properties of **oxa-1-7** and **S1b** studied in 50 mM PBS (pH 7.4)/DMSO (9:1) also gave comparable results when using CH_2Cl_2 as solvent. (Figures S2-S9 and Table S2, ESI†).

Table 2. Photophysical properties of **S1b** and **oxa-1-7** in CH_2Cl_2.[a]

Entry	Com-pound	Max. Abs (nm)	Max. Em (nm)	Sto-kes Shift (nm)	ε (M^{-1} cm^{-1})	λ_{ex} (nm)	Φ_F[a]
1	**S1b**	295	310	15	12100	270	0.06
2	**oxa-1**	363	413	50	22400	360	0.35
3	**oxa-2**	363	413	50	36900	360	0.33
4	**oxa-3**	365	480	115	68000	365	0.51
5	**oxa-4**	363	413	50	35200	360	0.34
6	**oxa-5**	380	425	45	42000	370	0.09
7	**oxa-6**	380	500	132	30700	365	0.40
8	**oxa-7**	380	430	50	46500	365	0.07

[a] Quantum yields were measured using coumarin 153 (Φ_F = 0.54 in ethanol) as the standard reference.

Based on the TD-DFT calculated electronic transitions, we simulated the absorption spectrum (Figure S10a, red line, ESI†) for **oxa-2**. The simulated spectrum resembles the measured spectrum. TD-DFT calculations reveal that the lowest energy absorption band ($\lambda_{abs,cal}$ = 341 nm) is originated from the HOMO→LUMO transition. The HOMO is mainly contributed by the π orbital of oxazolinium and phenyl rings, whereas LUMO is composed of the π * of oxazolinium ring (Figure 3). We have also simulated the emission spectrum (Figure S10b, red line, ESI†) for **oxa-2**, where calculated emission maximum ($S_1 \rightarrow S_0$ transition, $\lambda_{em,cal}$ = 436 nm) is close to the measured value (λ_{em} = 413 nm).

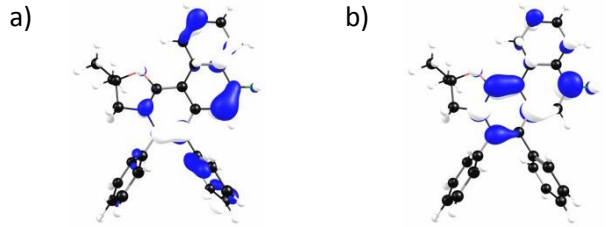

Figure 3. a) HOMO and b) LUMO of **oxa-2**, isovalue = 0.05.

Scope Study for Peptide Modifications

A substrate scope study was conducted utilizing **oxa-3** due to its possession of the highest quantum yield among other analogues. Various cysteine-containing peptides were treated with **oxa-3** under the optimized conditions (Table 3). Up to 90% conversion was observed when various cysteine-containing peptides were treated (entries 1-7). No conversion was observed when peptide **7** (without cysteine) was employed (entry 7), indicating excellent cysteine selectivity.

View Article Online DOI: 10.1039/D5CB00289G

Table 3. Scope study of different peptides with **oxa-3**.[a]

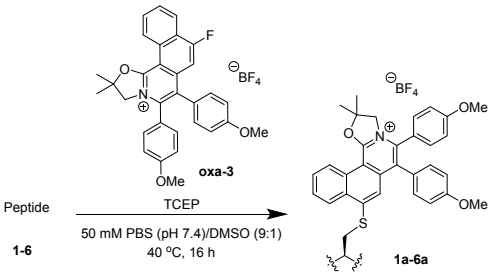

Entry	Peptide	Amino acid sequence	Product	Conv. (%)[b]
1	**1**	STSSSCNLSK	**1c**	90
2	**2**	AYEMWCFSQR	**2a**	69
3	**3**	KSTFC	**3a**	72
4	**4**	CSKFR	**4a**	89
5	**5**	CDPGYIGSR	**5a**	83
6	**6**	AYEMWCFHQR	**6a**	71
7	**7**	YTSSSKNVVR	**7a**	0

[a] Reaction conditions for modification: treatment of peptide (0.1 mM) with **oxa-3** (5 equiv.) in the presence of TCEP (1 equiv.) in 50 mM PBS buffer (pH 7.4)/DMSO (9:1) at 40 °C for 16 h. [b] Conversion was determined by LC-MS/MS analysis.

Modification of Proteins by Fluorescent Oxa-3

Next, **oxa-3** was utilized for protein modification of Bovine serum albumin (BSA; PDB ID: 4F5S) and human serum albumin (HSA; PDB ID: 1AO6) with a single free cysteine residue at position 34 (Cys-34), without TCEP to maintain structural integrity of proteins (Scheme 3). By LC-MS analysis, 60% conversion of **oxa-3**-modified BSA (Figures S53-54, ESI†) and 70% conversion of **oxa-3**-modified HSA (Figures S55-56, ESI†) were achieved after 16 h. Conversely, lysozyme (PDB ID: 3LYZ) remained intact after the reaction (Figures S57-58, ESI†).

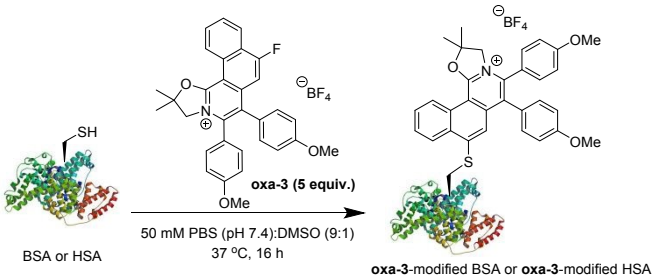

Scheme 3. S_NAr reaction of protein using **oxa-3**.

Analysis of protease-digested **oxa-3**-modified proteins showed that the reaction only occurred at Cys-34 of targeted peptide fragments, while other amino acid residues remained intact (Figures S59-64, ESI†). SDS-PAGE analysis revealed a strong blue fluorescent signal for **oxa-3**-modified proteins while no signal was observed for native BSA and HSA at UV 365 nm (Table 4). Coomassie blue staining on the same gel gave deep blue colour signals of all native and modified proteins, indicating successful cysteine arylation of proteins by **oxa-3**. Both native and treated lysozyme had no fluorescence, stipulating excellent site-selectivity for peptide and protein modification.

Table 4. SDS-PAGE analysis of **oxa-3**-modified proteins.

	UV 365 nm		Coomassie Blue	
Protein	-	+	-	+
BSA	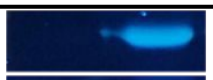		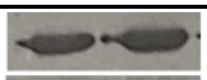	
HSA				
Lysozyme				

Live Cell Imaging

Following the success of **oxa-3** in the provision of visual indication in protein modification, we sought to explore its applicability for cell imaging in biological systems. Cytotoxicity of **oxa-3** and **oxa-6** was evaluated at 24 h showing moderate cytotoxicity to HeLa cells (IC_{50} = 16.11 and 14.54 µM, respectively, Figures S66-67, ESI†). Then, the colocalization subcellular imaging of **oxa-3** and **oxa-6** was investigated at a non-cytotoxic concentration. HeLa cells were incubated with oxazoliniums (5 µM) in the presence of MitoTracker Red (MTR, 500 nM) for 15 min and washed with DPBS before the confocal imaging. As shown in Figure 4, **oxa-3** and **oxa-6** showed remarkable cell permeability, intense green fluorescence, and good overlapping with MTR, with Pearson's correlation coefficient value close to 0.8 indicating that **oxa-3** and **oxa-6** localized in the mitochondria.

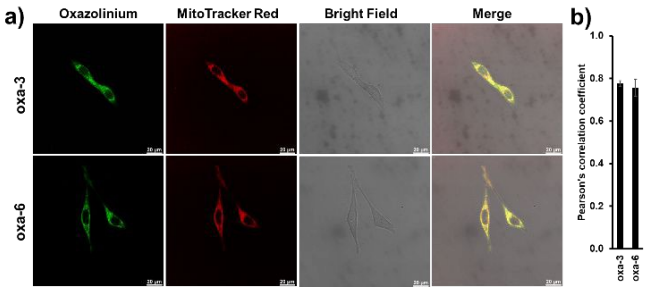

Figure 4. a) Live cell images of HeLa cells incubated with 5 µM **oxa-3** and **oxa-6** and 500 nM MTR for 15 min at 37 °C. First and second columns indicated the green and red channels for oxazoliniums and MTR respectively. Third column and last column indicated bright-field images and merged images from the three channels respectively. b) Pearson's correlation coefficient of colocalization between oxazoliniums and MTR.

Due to the high concentrations of glutathione (GSH, 1-10 mM) present in the cells,[27] we studied the reactivity of **oxa-3** with GSH by incubating **oxa-3** (1 mM) with GSH (1 mM) for 15 min. Our results showed that 31% conversion was observed,

indicating that the oxazoliniums have reactivity towards -SH containing biomolecules in cells (Figures S69-71, ESI†).

Conclusions

In conclusion, we have developed a series of fluorescent cationic fluorinated oxazoliniums for cysteine-selective arylation *via* S_NAr reaction. Measurements of photophysical properties and quantum yields presented **oxa-3**, with the electron-donating -OMe group, with a high quantum yield of 0.51. Under the optimized conditions, modifications of cysteine-containing peptides afforded up to 99% conversion. Finally, applicability of **oxa-3** to provide visual indication for fluorescent labelling of cysteine-containing proteins and cell imaging were successfully demonstrated. This work highlights the potential of these fluorescent oxazoliniums for broad applications in chemical biology and biological studies.

Author contributions

K. K.-Y. K. and Y. T. L.: conceptualization, investigation, data curation, writing – original draft, writing – review & editing; A. T.: investigation, formal analysis, writing – original draft; J.-R. D.: formal analysis, writing – original draft; L.-Y. T.: investigation; M.-K. W.: conceptualization, funding acquisition, supervision, writing – review & editing.

Conflicts of interest

There are no conflicts to declare.

Data availability

The data supporting this article have been included as part of the ESI.†

Acknowledgements

We gratefully acknowledge the financial support by the Research Grants Council of the Hong Kong Special Administrative Region, China (PolyU15300520), PolyU Postdoc Matching Fund Scheme (P0043412: W262), by the InnoHK initiative of the Innovation and Technology Commission of the Hong Kong Special Administrative Region Government, the State Key Laboratory of Chemical Biology and Drug Discovery, The Hong Kong Polytechnic University (P0053072: ZZV2), the University Research Facility in Life Sciences (ULS) and the University Research Facility in Chemical and Environmental Analysis (UCEA) of PolyU. We would like to thank Prof. F. K.-C. Leung from Department of Applied Biology and Chemical Technology (ABCT) of The Hong Kong Polytechnic University for hardware support of in vitro and cell imaging experiments.

References

1. C. D. Spicer and B. G. Davis, *Nat. Commun.*, 2014, **5**, 4740.
2. N. Stephanopoulos and M. B. Francis, *Nat. Chem. Biol.*, 2011, **7**, 876-884.
3. L. R. Malins, *Curr. Opin. Chem. Biol.*, 2018, **46**, 25-32.
4. S. B. Gunnoo and A. Madder, *ChemBioChem*, 2016, **17**, 529-553.
5. C. Zhang, E. V. Vinogradova, A. M. Spokoyny, S. L. Buchwald and B. L. Pentelute, *Angew. Chem. Int. Ed.*, 2019, **58**, 4810-4839.
6. W. Lin, X. Ding, J.-W. Han, L.-S. Yu and F.-J. Chen, *Org. Chem. Front.*, 2025, **12**, 2777-2789.
7. A. M. Spokoyny, Y. Zou, J. J. Ling, H. Yu, Y.-S. Lin and B. L. Pentelute, *J. Am. Chem. Soc.*, 2013, **135**, 5946-5949.
8. Y. Zou, A. M. Spokoyny, C. Zhang, M. D. Simon, H. Yu, Y.-S. Lin and B. L. Pentelute, *Org. Biomol. Chem.*, 2014, **12**, 566-573.
9. S. Kalhor-Monfared, M. Jafari, J. Patterson, P. Kitov, J. Dwyer, J. Nuss and R. Derda, *Chem. Sci.*, 2016, **7**, 3785-3790.
10. D. Gimenez, C. A. Mooney, A. Dose, G. Sandford, C. R. Coxon and S. L. Cobb, *Org. Biomol. Chem.*, 2017, **15**, 4086-4095.
11. W. Liu, Y. Zheng, X. Kong, C. Heinis, Y. Zhao and C. Wu, *Angew. Chem. Int. Ed.*, 2017, **56**, 4458-4463.
12. T. Tsunemi, S. J. Bernardino, A. Mendoza, C. G. Jones and P. G. Harran, *Angew. Chem. Int. Ed.*, 2020, **59**, 674-678.
13. B. M. Lipka, V. M. Betti, D. S. Honeycutt, D. L. Zelmanovich, M. Adamczyk, R. Wu, H. S. Blume, C. A. Mendina, J. M. Goldberg and F. Wang, *Bioconjug. Chem.*, 2022, **33**, 2189-2196.
14. S. Casa and M. Henary, *Molecules*, 2021, **26**, 1160.
15. S. Zeng, X. Liu, Y. S. Kafuti, H. Kim, J. Wang, X. Peng, H. Li and J. Yoon, *Chem. Soc. Rev.*, 2023, **52**, 5607-5651.
16. F. de Moliner, F. Nadal-Bufi and M. Vendrell, *Curr. Opin. Chem. Biol.*, 2024, **80**, 102458.
17. G.-Q. Jin, J.-X. Wang, J. Lu, H. Zhang, Y. Yao, Y. Ning, H. Lu, S. Gao and J.-L. Zhang, *Chem. Sci.*, 2023, **14**, 2070-2081.
18. P. Gandeepan and C. H. Cheng, *Chem. Asian J.*, 2016, **11**, 448-460.
19. P. Karak, S. S. Rana and J. Choudhury, *Chem. Commun.*, 2022, **58**, 133-154.
20. R. Sanjana, J. Jayakumar and K. Parthasarathy, *Asian J. Org. Chem.*, 2025, e202500177.
21. C. Z. Luo, P. Gandeepan, J. Jayakumar, K. Parthasarathy, Y. W. Chang and C. H. Cheng, *Chem. Eur. J.*, 2013, **19**, 14181-14186.
22. J.-R. Deng, W.-C. Chan, N. C.-H. Lai, B. Yang, C.-S. Tsang, B. C.-B. Ko, S. L.-F. Chan and M.-K. Wong, *Chem. Sci.*, 2017, **8**, 7537–7544.
23. W.-M. Yip, Q. Yu, A. Tantipanjaporn, W.-C. Chan, J.-R. Deng, B. C.-B. Ko and M.-K. Wong, *Org. Biomol. Chem.*, 2021, **19**, 8507-8515.
24. A. Tantipanjaporn, K.-Y. K. Kung, J.-R. Deng and M.-K. Wong, *Spectrochim. Acta - A: Mol. Biomol. Spectrosc.*, 2024, **319**, 124524.
25. L.-Y. Tsang, A. Tantipanjaporn, K. K.-Y. Kung, H.-Y. Sit, W.-Y. O, A. K.-H. Chan, N. C.-H. Lai and M.-K. Wong, *Adv. Synth. Catal.*, 2025, **367**, e70023.
26. M. N. Holerca and V. Percec, *Eur. J. Org. Chem.*, 2000, **2000**, 2257-2263.
27. C.-Y. Cui, B. Li and X.-C. Su, *ACS Cent. Sci.*, 2023, **9**, 1623-1632.

View Article Online
DOI: 10.1039/D5CB00289C

Data availability

The data supporting this article have been included as part of the ESI.†